Developments in the Built Environment 17 (2024) 100316

Contents lists available at ScienceDirect

Developments in the Built Environment

journal homepage: www.sciencedirect.com/journal/developments-in-the-built-environment

Maximizing the use of recycled aggregates from combined thermal/mechanical and accelerated carbonation treatment

Bruno Wenzel [a], Viviana Letelier [a,b,*], Gonzalo Zambrano [a], Marión Bustamante [c], José Marcos Ortega [d]

[a] Department of Civil Engineering, Universidad de La Frontera, Temuco, 4780000, Chile
[b] Biotechnological Research Center Applied to the Environment (CIBAMA-BIOREN), Universidad de La Frontera, Temuco, 4780000, Chile
[c] Doctoral Program in Engineering at the MacroFacultad de Ingeniería UFRO-UBB-UTAL, Temuco, 4780000, Chile
[d] Departamento de Ingeniería Civil, Universidad de Alicante, Alacant, 03080, Spain

ARTICLE INFO

Keywords:
Recycled aggregates
Concrete
Thermal/mechanical treatment
Accelerated carbonation

ABSTRACT

The global emphasis on using recycled concrete aggregates (RCA) to reduce the depletion of natural resources has grown significantly. However, the presence of adhered mortar limits their usage in concrete to the coarse fraction and at low replacement rates, as complete replacement remains a challenge. This study aims to improve concrete with low-quality recycled aggregates through thermal/mechanical treatment combined with accelerated carbonation. Physical, chemical and mechanical properties of concretes with 100% coarse and fine RCA were evaluated. Results revealed that after the combined treatment the water absorption of coarse and fine RCA decreased by 18% and 6%, respectively. SEM images showed the precipitation of calcite with better crystallinity, resulting in a denser cement matrix, although water absorption and porosity were slightly improved. Furthermore, compressive and flexural strength of treated concrete achieved 91% and 96% of the control series, considering full RCA replacement and a higher w/c ratio.

1. Introduction

In the last four decades the world population living in cities has doubled, reaching 3.5 billion in 2015 (OECD and European Commission, 2020). As a result of this urban growth, new infrastructure must be built to meet the various needs of this sector's growing population, including the construction of new bridges, buildings, roadways and dams, among other civil works. However, these works lead to a large consumption of materials, which is why the construction industry reaches 40% of the annual use of these materials globally (David et al., 2018). Hence, the extraction of natural aggregates (NA) was nearly 50 billion tons in 2017, with an estimated increase to 60 billion tons by 2030 (Tam et al., 2021). In addition, an estimated of 15 billion tons of sand is consumed every year, which has led to unsustainable use of river sand and a shortage of this resource (Cao et al., 2022; Liu et al., 2021a). On the other hand, the construction industry generates a large amount of waste from these processes, and together with the demolition industry, they are the main producers of solid waste worldwide, generating approximately 30–40% of the annual total (Islam et al., 2019). As a result, there is a need to create a circular economy that can reduce the use of new natural resources, and that can valorize the reuse of the different wastes generated in the construction and demolition industries. In addition, based on the Paris Agreement on climate change many countries are focused on achieving zero carbon (Makul, 2020), thus leading to the development of new technologies for carbon capture, utilization and storage, in order to reduce CO_2 emissions of construction materials (Han et al., 2023).

Among the solutions to mitigate the problems described is the replacement of NA by recycled concrete aggregate (RCA). However, RCA has lower quality properties than natural aggregate because the material extracted from the rubble has mortar adhered to it, which implies different disadvantages when used. These disadvantages include the decrease in density, increase in water absorption, abrasion loss percentage and crushing ratio, presence of organic impurities, and presence of hazardous chemical substances, among others (Malešev et al., 2010). In addition, it should be noted that the finer the RCA, the greater the presence of adhered mortar, and therefore the performance of its properties will be increasingly compromised. For this same reason, various international standards that have begun to approve the use of

* Corresponding author. Department of Civil Engineering, Universidad de La Frontera, Temuco, 4780000, Chile.
E-mail address: viviana.letelier@ufrontera.cl (V. Letelier).

https://doi.org/10.1016/j.dibe.2023.100316
Received 25 August 2023; Received in revised form 21 November 2023; Accepted 26 December 2023
Available online 29 December 2023

RCA limit it only to the coarse fraction for structural concretes (Gonçalves and De Brito, 2010). Hence, several studies have focused on improving the quality of RCA, where eliminating the adhered mortar or improving its microstructure is the objective (Castellote et al., 2009; Al-Bayati et al., 2016; Wang et al., 2016; Xuan et al., 2016; Zadeh et al., 2021).

To eliminate the mortar attached to the aggregates several treatments have been studied. Among them, the mechanical treatment removes the adhered mortar trough abrasion in a Los Angeles (LA) machine or Micro-Deval device. On the other hand, thermal and chemical treatments weaken the structure of the adhered mortar, which can then be removed by some type of mechanical treatment (Pandurangan et al., 2016; Tanta et al., 2022). Thus, the thermal treatment can dehydrate and weaken the structure of the adhered mortar by the chemical decomposition generated during the treatment. These processes create microfissures in the adhered mortar, which helps in its removal by mechanical treatment (Pandurangan et al., 2016; Prajapati et al., 2021). Sui and Mueller (2012) reported that moderate temperatures of 250–300 °C are sufficient to remove the adhered mortar if followed by an intensive mechanical treatment, but temperatures of 500 °C followed by a short mechanical treatment can take advantage of the cement paste enriched powder and use it as a hydraulic binder. Moreover, the thermal expansion difference within the temperature range of 400–500 °C promotes preferential fracture of the mortar-aggregate interface due to the decomposition of portlandite and the dehydration of C–S–H (Prajapati et al., 2021; Zhang et al., 2022). On the other hand, when the RCA is exposed to higher temperatures between 600 and 800 °C, the cement matrix exhibits severe microcracking due to the decarbonation process, which leads to the degradation and mass loss of the aggregate, facilitating the removal of the adhered mortar (Al-Bayati et al., 2016). According to Wang et al. (2017), C–S–H decomposes into β-C_2S at 600–700 °C, resulting in severe deterioration of mechanical properties of mortar. Considering the above, studies that have implemented the mechanical treatment have concluded that as the treatment temperature increases, there is a greater elimination of the mortar, but that after 500 °C the water absorption of the material increases, which is why this is considered an optimal temperature for the elimination of adhered material and reduction in water absorption (Al-Bayati et al., 2016; Pepe et al., 2014).

Another option to improve the quality of recycled aggregate is to improve its microstructure, where the accelerated carbonation process has shown good results in previous studies, since the chemical composition of the adhered mortar has the capacity to react with CO_2 (Zadeh et al., 2021; Morandeau et al., 2014; Shi et al., 2018; Zhan et al., 2020; Wang et al., 2022). Some of the reactive components are portlandite ($Ca(OH)_2$) and calcium silicate hydrate (C–S–H). The former is one of the main components produced during cement hydration and slowly reacts with the CO_2 in the atmosphere to form calcite ($CaCO_3$) plus H_2O. This process causes an increase in the volume of mortar, which also contributes to filling the pores present in it, thus densifying the aggregate and reducing the water absorption of the material. On the other hand, C–S–H is able to react with the CO_2, generating $CaCO_3$ plus H_2O like the portlandite, but in a milder and less significant way when assessing material improvements (Zhan et al., 2014). However, the effectiveness of this process will depend on different factors, some of which are the amount of portlandite and C–S–H present in the aggregate, the environmental conditions of relative humidity and temperature to which the material is exposed, the CO_2 concentration, the pressure with which it is injected, and the duration of this process (Castellote et al., 2009; Hyvert et al., 2010; Šavija and Luković, 2016; Lu et al., 2019).

Currently, few authors have focused their studies on the effect of combined treatments to improve the properties of recycled aggregates (Al-Bayati et al., 2016; Kazmi et al., 2019, 2020, 2021; Munir et al., 2021; Rostami et al., 2021). Among them, Kazmi et al. (2019) investigated the mechanical behavior of concretes containing RCA treated by carbonation, acetic acid immersion with mechanical rubbing, acetic acid immersion with carbonation and lime immersion with carbonation. After all treatments the physical properties of RCAs were improved. Moreover, concretes with RCA treated through acetic acid immersion with mechanical rubbing and lime immersion with carbonation obtained stress-strain curves very close to the NA concrete. On the other hand, Rostami et al. (2021) evaluated the effect of paraffin coating and aerogel aggregates on cement composites. Their results indicate that paraffin coating improved durability properties but decreased compressive strength of the mixtures, while adding aerogel aggregates the thermal conductivity is significantly improved.

Most of the studies use treatments separately, mainly in the coarse fraction of good quality RCA in small quantities while the fine fraction is usually discarded. Therefore, the objective of this study is to improve the performance of concrete made with 100% low-quality coarse and fine recycled aggregate (CRA and FRA, respectively) from a single source, i.e. non-structural concrete partially carbonated due to weathering, by implementing two treatments together. The recycled aggregates were first subjected to a high temperature to facilitate the mechanical removal of the adhered mortar, and then were subjected to an accelerated carbonation process. In order to study their behavior, the RCA before and after the treatments were characterized and compared to the NA. Subsequently, tests were performed to assess the mechanical, physical, chemical and microstructural properties of concretes, which were compared to those of conventional concrete to evaluate its potential and feasibility. Moreover, this could increase the utilization of RCA as an environmentally friendly solution in the construction industry, especially the fine fraction considering the current global scarcity of fine NA.

2. Materials and characteristics

2.1. Cement

The cement used in this study is formulated on the basis of clinker, pozzolana and plaster. The classification of this cement according to ASTM C595/C595M − 21 (ASTM C595/C595M − 16, 2021) is Type IP (Portland-pozzolana cement). According to its data sheet, it has an initial setting time of 180 min and a final setting time of 240 min, a specific Blaine surface area of 4100 cm^2/g, and a specific weight of 2.81 g/dm^3. It has compressive and tensile strengths at 7 days of 230 kg/cm^2 and 45 kg/cm^2, respectively; at 28 days of 340 kg/cm^2 and 62 kg/cm^2, respectively.

2.2. Aggregates

The coarse and fine natural aggregates (CNA and FNA, respectively) are of siliceous origin and come from a local aggregate plant in southern Chile, while the coarse and fine recycled aggregates (CRA and FRA, respectively) come from concrete fence panels with a compressive strength of 20 MPa, demolished and provided by a company that makes precast concrete in the area, which were crushed to obtain the desired sizes. In addition, the recycled aggregates were first subjected to a thermal/mechanical treatment (CRA-T and FRA-T), and then in combination to an accelerated carbonation process (CRA-TC and FRA-TC). The properties of both natural and recycled aggregates, in addition to the treated RCA, appear in Table 1, while the granulometry of the aggregates used is presented in Fig. 1. It is worth noting that the provided concrete fence panels had a prolonged exposure to the weather, so a natural carbonation process occurred when the hydration components of the cement matrix reacted with the atmospheric CO_2, transforming into calcite.

2.3. Superplasticizer (SP)

A superplasticizer (SP) was used in all the concrete series to obtain a mixture with greater plasticity and a smaller amount of mixing water to

Table 1
Physical properties of the aggregates.

Aggregate type	Specific gravity (OD)	Specific gravity (SSD)	Apparent specific gravity	Water absorption (%)	LA abrasion loss (%)
CNA	2.69	2.65	2.75	1.40	19.93
FNA	2.54	2.48	2.62	2.17	–
CRA	2.44	2.27	2.72	7.19	37.94
FRA	2.32	2.14	2.60	8.41	–
CRA-T	2.45	2.30	2.70	6.40	45.56
FRA-T	2.34	2.18	2.59	7.40	–
CRA-TC	2.46	2.32	2.69	5.90	42.36
FRA-TC	2.37	2.20	2.66	7.89	–

facilitate the workability of the concrete mixtures and avoid reducing its strength. The SP is classified as Type F according to ASTM C494/C494M – 19 (ASTM C494/C494M – 19, 2019) and has a specific gravity of 1.20 ± 0.02 kg/l. To obtain an effective use of the additive, this was added in the maximum allowable percentage of 2% by weight of the cement used and the entire fine aggregate mesh was increased by 10% according to the data sheet to maintain the homogeneity and consistency of the mixture.

3. Experimental program

3.1. Treatments of RCA

Regarding the improvement methods of the recycled aggregates used in this study, after crushing, the CRA was first subjected to a thermal treatment in a muffle furnace at 500 °C for 2 h, so that the adhered mortar structure is weakened. After the time had elapsed, the CRA was removed from the muffle and left to cool slowly at room temperature. Then, the loosened adhered mortar was removed using the Los Angeles abrasion machine using twelve 46 mm steel balls weighing 390 g and six smaller 20 mm steel balls weighing 33 g for a duration of 10 min, corresponding to 300 revolutions at 30 rpm. The purpose of the two different diameter steel balls and the 300 revolutions used in this treatment instead of the procedure specified in the ASTM C131/C131M – 20 (ASTM C131/C131M – 20, 2020) is to optimize the treatment without damaging the aggregates to which the mortar is adhered. From this same process, the RCA was screened to obtain the fine fraction of the RCA (FRA). After the first treatment was done, the RCA was subjected to a process of CO_2 injection for 6 h under controlled conditions of material humidity (5%), relative humidity (50 ± 5%), temperature (20 °C) and pressure (80 mbar). Once both treatments were done, the RCA was stored in a suitable environment to collect the required amount for the manufacture of the concrete series.

3.2. Mixture proportions

The concrete mixture was designed for a strength of 30 MPa and a fluid consistency to obtain a suitable workability. Three series were included for this study. A first control series (C00) was made entirely with NA, and then a series with 100% replacement with coarse and fine RCA with thermal treatment and carbonation (RCA-TC100). Cylindrical and prismatic specimens were included for both series, whereas for the final series (RCA100) only cylindrical specimens were made with a 100% replacement by untreated RCA to compare the most significant results and analyze the effect of the treatment used. In this way, we seek to obtain results under the most unfavorable conditions in order to draw relevant conclusions from them.

All the series were made based on the NA granulometry provided in Fig. 1 and the proportions of each are detailed in Table 2. The coarse and fine aggregates (RCA and NA) were first oven dried and initially all mixtures were made with a w/c ratio of 0.48. However, considering the high water absorption of the recycled aggregates, additional water was added to the mixing in order to maintain a consistent level of workability, with a slump in the range of 90 ± 5 mm for all mixtures to obtain a fluid consistency and fulfill the needs of the industry; thus, the w/c ratio from Table 2 corresponds to initial water plus additional water. In addition, the use of the SP helped to obtain mixtures with better plasticity and to keep the slump within the specified range.

3.3. Test methods

3.3.1. Characteristics of the aggregates

The characterization of coarse and fine aggregates (i.e., specific gravity and water absorption) of both natural and recycled aggregates (treated and untreated) was determined according to ASTM C127-15 (ASTM C127-15, 2015) and ASTM C128-15 (ASTM C128-15, 2015), respectively. In addition, the Los Angeles abrasion loss was determined according to ASTM C131/C131M – 20 (ASTM C131/C131M – 20, 2020).

3.3.2. Compressive strength and modulus of elasticity

The compressive strength of the concrete specimens was determined according to specifications in ASTM C39/C39M – 21 (ASTM C39/C39M – 21, 2021). The specimens for each series were cured for 7 and 28 days

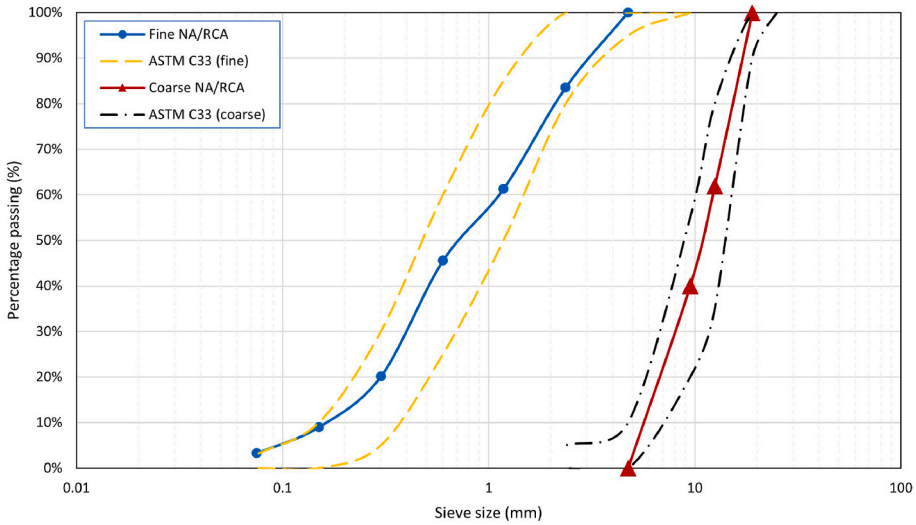

Fig. 1. Particle size distribution used for NA and RCA.

Table 2
Mix proportions of concrete (kg/m^3).

Sample	Water	Extra water	Cement	w/c	FNA	FRA	FRA-TC	CNA	CRA	CRA-TC	SP
C00	184	–	382	0.48	702	0	0	1061	0	0	7.65
RCA100	184	110	382	0.77	0	702	0	0	1061	0	7.65
RCA-TC100	184	95	382	0.73	0	0	702	0	0	1061	7.65

according to ASTM C31/C31M − 19 (ASTM C31/C31M − 19, 2019). Cylindrical specimens of 15 cm in diameter and 30 cm in height were made and tested for each curing time. The test was performed in the testing machine at a continuous loading rate of 0.25 MPa ± 0.05 MPa until the specimen ruptured.

Along with the compressive strength test, the modulus of elasticity was determined for the cylindrical specimens after 28 days of curing according to specifications in ASTM C469/C469M − 14 (ASTM C469/C469M − 14, 2014). This test includes the compressive stress to which the specimen is subjected as well as the vertical and horizontal deformations, which are measured with the aid of a standard extensometer.

3.3.3. Flexural strength

The concrete specimens were subjected to a flexural strength test according to the specifications in ASTM C78/C78M − 18 (ASTM C78/C78M − 18, 2018). Prismatic specimens of 15 cm × 15 cm × 55 cm per series were tested after 28 days of curing. The specimens were placed in the testing machine, continuously applying a P/2 load at both upper load application points until the fracture of the specimens.

3.3.4. Density, absorption and porosity

For each series, the density, water absorption and porosity were determined using ASTM C642-21 (ASTM C642-21, 2021). Specimens of 10 cm in diameter and 20 cm in height with 28 days of curing were made, which were then cut into 10 cm × 5 cm slices. From these, the submerged, saturated and dry masses were determined to then make the relevant calculations.

3.3.5. Capillary absorption

The water absorption rate was calculated according to the specifications in ASTM C1585-20 (ASTM C1585-20, 2020). For each series, slices of 10 cm in diameter and 5 cm in height with 28 days of curing were used for each series. The upper side and the lateral surface of the specimens were waterproofed in order to obtain the absorption rate only on the underside of the specimens. The increase in mass of the specimens was recorded from 1 min to 6 h and the initial capillary absorption was determined for each series.

3.3.6. Thermal conductivity and thermal diffusivity

The thermal conductivity and thermal diffusivity properties of the concrete were obtained through a test conducted as indicated in ISO 22007–2 (ISO 22007–2:2008(E), 2008). Specimens of 10 cm in diameter and 5 cm in height for each series with 28 days of curing were tested. In addition, prior to the test, the samples were conditioned and maintained at a room temperature of 20 °C. The measurements were taken with the Hot Disk TPS 1500, which records the temperature gradients and provides thermal conductivity and thermal diffusivity among its results.

3.3.7. Ultrasonic pulse velocity (UPV)

To measure the homogeneity of the concrete, the ultrasonic pulse velocity (UPV) test was conducted according to ASTM C597-16 (ASTM C597-16, 2016). The specimens used were cured for 28 days, and were 10 cm in diameter and 5 cm in height. For the measurements, a CONTROLS PULSONIC 58-E4900 analyzer was used to detect the time it takes for a pulse to pass through a sample of a given thickness. Finally, the velocity of the pulse was determined based on the distance covered and the time elapsed.

3.3.8. Scanning electron microscope (SEM)

The analysis of the concrete microstructure was based on images taken with a scanning electron microscope (SEM), which is equipped with a backscattered electron (BSE) image detector and an energy dispersive spectrometer (EDS). These images were processed using a HITACHI SU3500, with a voltage of 10 kV and a working distance of 12 ± 0.2 mm.

3.3.9. X-ray diffraction (XRD)

The XRD analyses were carried out with the Bruker D2 PHASER employing an X-ray tube (Cu 1.54 Å). The diffraction pattern was obtained over a 2θ range of 10°–80°, with a duration of 60 min and a rate of 1 s. Before the test was conducted, the samples were subjected to a conditioning process to obtain dust particles smaller than 75 μm.

3.3.10. Thermogravimetric analysis (TGA)

The thermogravimetric analysis (TGA) was done with a heating speed of 20 °C/min for 10 min until reaching 1000 °C, recording the mass variation in the samples during the test using a Q600 SDT from TA Instruments. From these measurements the TGA curve is obtained, and with this the first derivative of the mass loss during the temperature increase (DTG) is determined. This curve makes it possible to discern different peaks associated with the variation in the H_2O and CO_2 emissions (Morandeau et al., 2014).

3.3.11. CO_2 uptake

Accelerated carbonation is a very complex process due to the reaction that occurs, the physicochemical characteristics, the atmospheric exposure to CO_2 where the samples are located, and the influence of the kinetics of the process. For this, the absorption of CO_2 in the concrete samples was evaluated through the mass loss resulting from the thermogravimetric analysis associated with decarbonation. Despite the varied literature based on Equation (1) indicated by Zhang et al. (2017) in their bibliographical review, there are differences among the authors due to the range of temperatures used. This is because from this mass loss, the sequestered CO_2 can be estimated by considering the amount of $CaCO_3$ present in the concrete sample. In this case, Equation (2) proposed by Kaliyavaradhan et al. (2020) is used, where Δm_{CO_2} represents the mass loss of the carbonated concretes in the temperature range of 540–950 °C (Qin and Gao, 2019) and $m_{105°C}$ the dry mass of the sample at 105 °C.

$$CO_2\ uptake\ (\%) = \frac{mass\ of\ reacted\ CO_2}{mass\ of\ CO_2\ reactive\ materials} \times 100 \quad (1)$$

$$CO_2\ (wt\%) = \frac{\Delta m_{CO_2}}{m_{105°C}} \times 100 \quad (2)$$

4. Results and discussion

4.1. Characteristics of the aggregates

The physical properties of the aggregates (i.e., specific gravity, water absorption and LA abrasion loss) are presented in Table 1. With respect to the specific gravity, the greatest variation was up to 14.34% less (SSD) for the untreated CRA compared to the NA. Although the differences are not very significant, it was possible to achieve a slight improvement in the aggregate with the thermal/mechanical treatment, and improve it even further after accelerated carbonation. On the other hand, the water

absorption of the CRA is 5.1 times greater than that of the coarse natural aggregate (CNA), although it decreases to 4.2 times after the application of both treatments, whereas for the fine portion these increases are between 3.9 and 3.4 times the absorption of the natural aggregate, respectively. Moreover, after carbonation of the thermal treated aggregates, there was a 6.6% increase in water absorption which may be due to the process parameters. Gholizadeh-Vayghan et al. (2020) indicate that carbonation under humid conditions or in a humid atmosphere does not lead to any improvement in water absorption, porosity or microstructure, regardless of CO_2 pressure and temperature. This could lead to leaching of the portlandite from the surface, resulting in an increase in RCA porosity and thus water absorption.

The LA abrasion loss was twice as high for the CRA compared to the CNA, where the treated aggregates experienced a slightly greater loss mostly due to the thermal/mechanical process, which dehydrates and weakens the mortar adhered to the aggregate at 500 °C, creating microfissures and thereby facilitating its removal with the LA abrasion machine. Similar behavior was noted by other authors (Al-Bayati et al., 2016; Alqarni et al., 2021). In addition, as mentioned in Section 3.1, the number of revolutions used in the mechanical treatment can lead to a weakening of the microstructure of the RCA (Alqarni et al., 2021); therefore, since a higher number of revolutions was not used so as not to weaken the microstructure too much, some mortar remained adhered to the RCA. It is also worth noting that after the first treatment, the accelerated carbonation was able to densify the microstructure of the RCA (Liu et al., 2021b), thereby reducing the LA abrasion loss.

These variations, especially in high water absorption, are attributed to the inferior RCA quality and the adhered mortar content (although in a smaller amount after the thermal/mechanical treatment), which consequently results in more pores and voids than natural aggregate. It should be noted that the thermal treatment allows a partial reactivation of the adhered mortar, which helps to enhance the cement matrix of the aggregates, thus improving the surface suitable for carbonation and obtaining a more effective replacement of the aggregates, including the fine fraction. This is because the thermal treatment dehydrates the cement hydration products such as C–S–H and $Ca(OH)_2$ (Carriço et al., 2020), leaving some space available for them to react again with the accelerated carbonation process and improve the microstructure between the adhered mortar and the RCA (Morandeau et al., 2014).

4.2. Compressive strength

The compressive strength results measured at 7 and 28 days are shown in Fig. 2. The series with NA (C00) has the highest compressive strength, followed by the series with treated RCA (RCA-TC100), and finally the series with untreated RCA (RCA100) had the lowest strength. For the case of the RCA-TC100 series, an average strength of 27.52 MPa was obtained at 28 days, which corresponds to 91.73% of the strength obtained for the control series (30 MPa); whereas for the RCA100 series, a strength of 21.95 MPa was achieved, which corresponds to 73.17% of the control series. The decrease in compressive strength of the series with recycled aggregates compared to the series with natural aggregates is influenced by the higher water quantity needed to maintain a good workability, which means a greater w/c ratio (Zega and Maio, 2009; Robalo et al., 2021). Despite this, the comparison between the strengths obtained for the treated and untreated recycled series showed an improvement of 25% after the combined treatment, which is in accordance with previous studies (Xuan et al., 2016; Tanta et al., 2022) where recycled aggregates treated separately with thermal and carbonation treatments obtained strengths 17% and 6.6% better than the untreated series, respectively. In addition, the strengths of the treated RACs were able to reach about 90% of the control series, consistent with the results obtained in this study. It is worth noting that although the w/c ratio of the RCA-TC100 series was 52.1% higher than that of the control series, thanks to the treatments carried out, it was 5.2% lower than that of the RCA100 series and the impact on the compressive strength was minimal

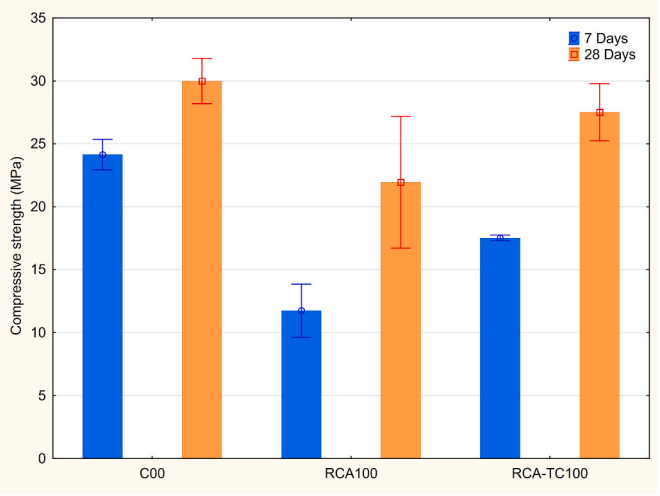

Fig. 2. Compressive strength at 7 and 28 days.

considering the unfavorable conditions of the mixtures, demonstrating the improvement obtained with the combined treatment compared to the untreated series.

Some authors attribute this increase in compressive strength between the treated and untreated series to the densification of the RCA. In this case, the thermal/mechanical treatment reduced the amount of mortar adhered to its surface and therefore its porosity. In addition to this and consistent with the results of the TGA analysis, carbonation was responsible for reinforcing this surface, achieving a greater density of the recycled material (Xuan et al., 2016; Tanta et al., 2022; Šavija and Luković, 2016). Densification can be seen in the SEM images in Fig. 3, where in (a) there is a greater number of pores in the adhered mortar and a more irregular interfacial transition zone (ITZ), whereas in (b) many of the pores were sealed by the carbonation process, and the ITZ between the RCA and the cement matrix has more regular contact due to the thermal process and later mechanical and carbonated abrasion.

4.3. Modulus of elasticity

The modulus of elasticity of the each series was determined along with the compressive strength test at 28 days, the results of which are in Fig. 4. From this, a 33.64% reduction is observed for the RCA100 and 26.64% for the RCA-TC100 compared to the C00. This decrease in the modulus of elasticity is due to the microfissures present in the RA and to its interface with the adhered mortar, which leads to a reduction in the rigidity of the system (Thomas et al., 2018). Zega and Maio (2009) had similar results for concretes with siliceous aggregates with a w/c ratio of 0.70, where the modulus of elasticity of the RAC was 25% less than the NAC.

On the other hand, it was possible to achieve a 10.55% increase for the RCA-TC100 series over the RCA100, which indicates that the combined treatment was able to improve the quality of the RA and the ITZ of the cement paste with adhered mortar (Neville, 1995). This agrees with the report by Kou et al. (2014) and Xuan et al. (2017), where the concrete with RA treated by accelerated carbonation was 13% higher than the untreated RA.

4.4. Flexural strength

The flexural strength of the C00 and RCA-TC series at 28 days appears in Fig. 5. These results show close strengths, where the series with treated RCA obtained a strength 3.96% lower than the control series, which coincides with Tanta et al. (2022) and Xuan et al. (2016), who obtained slightly lower strengths of 92% under the control series with RACs with thermal treatment and carbonated separately. This slight

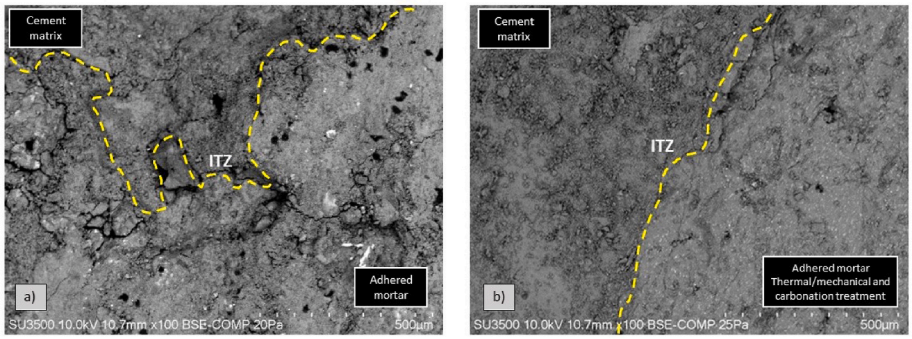

Fig. 3. SEM images of concrete at 28 days. (a) RCA100 series, and (b) RCA-TC100 series.

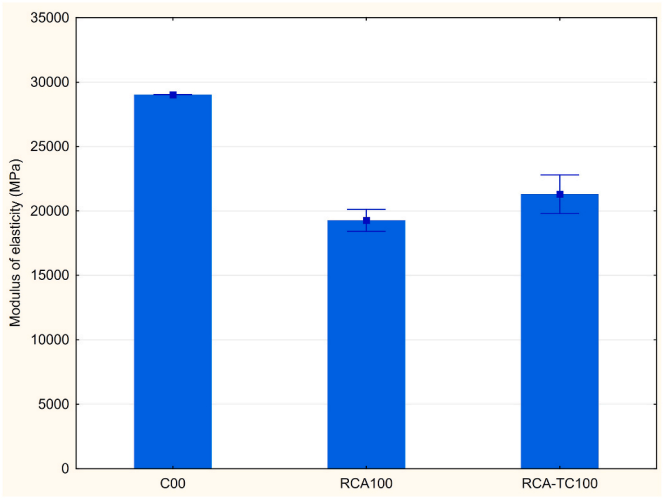

Fig. 4. Modulus of elasticity at 28 days.

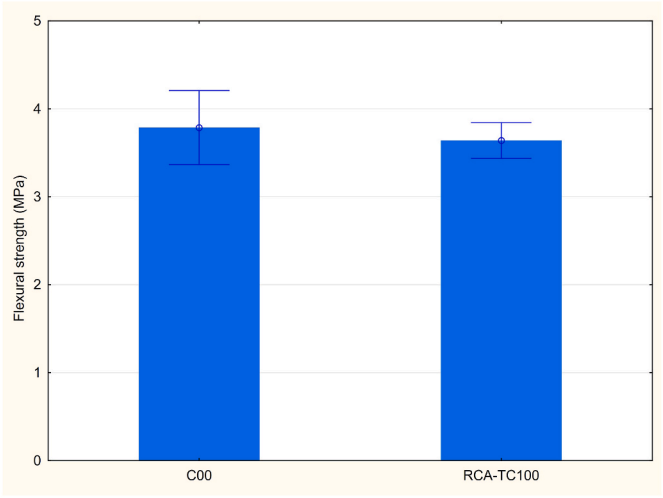

Fig. 5. Flexural strength at 28 days.

reduction in flexural behavior is due to the same phenomenon of densification and reduction in porosity resulting from the treatments that helped improve the compressive strength in Section 4.2 (Xuan et al., 2016; Tanta et al., 2022; Šavija and Luković, 2016).

4.5. Density, absorption and porosity

Fig. 6 illustrates the density, water absorption and porosity with 28 days of curing. It is noted that the density decreases with the replacement of RCA for NA up to 10.34%, and that there is also a slight increase in the concrete with RCA-TC compared to the RCA100 series corresponding to 1.92%. Porosity and water absorption, on the other hand, showed the opposite trend, also related to the reduction in density, where the RCA100 and RCA-TC100 series had porosities 46.25% and 42.98% and absorptions 62.70% and 56.75% greater than the control series, respectively.

The densification and improvement in the properties of both the aggregate and the recycled concrete are a consequence of the combination of the treatments used in this study. On the one hand, there is the elimination of the adhered mortar through the thermal/mechanical treatment, and then the densification of the remaining mortar from chemical processes resulting from carbonation. First, the adhered mortar is eliminated, which according to a study by Zhang et al. (2022), the efficiency in the microcracking of the adhered mortar increases as the material is exposed to higher temperatures, this being most evident at 500 °C as a result of the dehydration of the C–S–H and the chemical decomposition of the portlandite. This microcracking leads to the adhered material being eliminated by the thermal treatment, leading to a reduction in the relation of the volume between the mortar and the aggregate, causing an increase in its density. Shui et al. (2009) indicates that the densification produced after the thermal process is due to the rapid rehydration of the dehydrated components, making it possible to fill the empty spaces quickly and thus reduce the number of pores. In this study, after the thermal process and abrasion of the aggregates, they were hydrated with 5% water in relation to the weight of the material to be carbonated, resulting in a more densified matrix. This is noted when comparing the SEM images from the series without treatments (see Fig. 7) and the series with treatments (see Fig. 8). On the other hand, Šavija and Luković (2016) report that the reduction in the porosity can take place by carbonation of the C–S–H, which can be transformed into amorphous silica gel or calcite. This will depend on the existing calcium-silica ratio, where a reduction in this ratio will indicate a change in the C–S–H, which is transformed into an amorphous phase of silica gel, and which will also see a reduction in the amount of calcite produced. It is for this reason that for the case of the series being studied, densification may be attributed to the generation of the amorphous silica gel mentioned, as can be seen in Fig. 9, where in (a) the Ca/Si ratio of the RCA100 series is less than in (b), where the RCA-TC100 series presents a reduction in the ratio with the increase in silica.

4.6. Capillary absorption

The initial water absorption rates at 28 days are detailed in Fig. 10. From this it is noted that the C00 series obtained the smallest absorption rate in the first 6 h, followed by the RCA100 series with a 20% increase

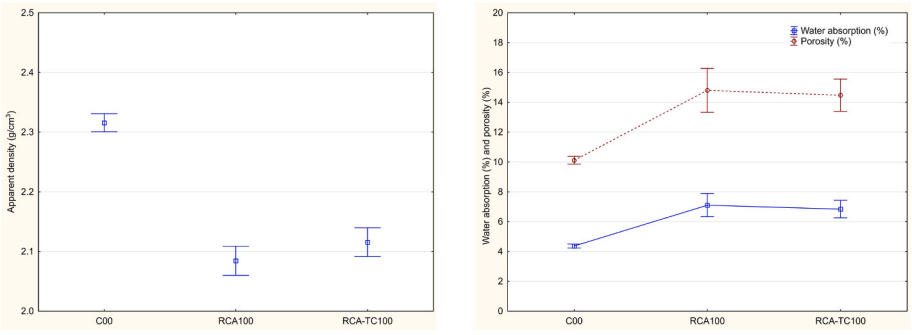

Fig. 6. (A) Apparent density, and (b) water absorption and porosity at 28 days.

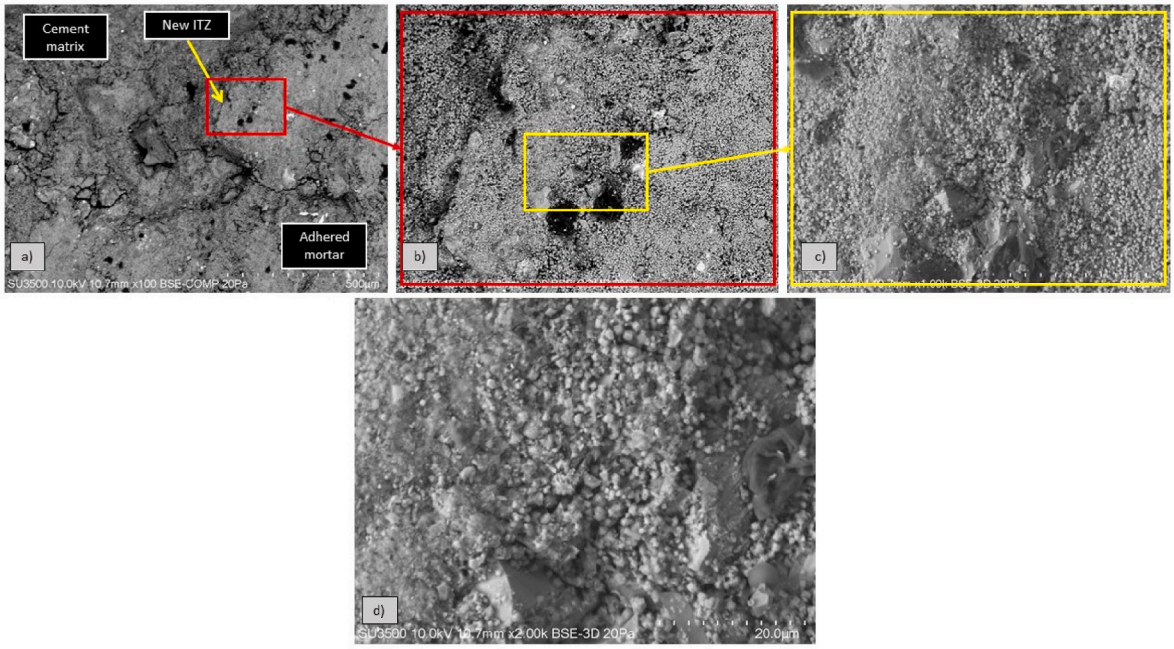

Fig. 7. SEM images of RCA100 series.

and the RCA-TC100 series with a 36% increase. According to Biskri et al. (2017), the increase in capillary absorption rates will depend on the existing capillary voids. Hence, the series with recycled material replacement present higher rates than the series with NA because they have a higher porosity. Despite the treated RCA series having less porosity than the untreated series, this presented greater capillarity, which could be due to the dehydration process undergone by the RCA due to the thermal treatment.

4.7. Thermal conductivity and thermal diffusivity

The thermal conductivity and thermal diffusivity with 28 days of curing are shown in Fig. 11. For both properties, the C00 series obtained the highest values, which decreased by up to 23.20% for the thermal conductivity and 12.82% for the thermal diffusivity when the NA was replaced by the RCA. This is linked to the decrease in density and the increase in the number of pores according to the study by Letelier et al. (2021). Since the change in the density and porosity between the RCA100 and RCA-TC100 series was not very significant as mentioned in Section 4.5, the improvement in the thermal conductivity and thermal diffusivity was less than 2.08% and 1.45%, respectively.

4.8. Ultrasonic pulse velocity (UPV)

Fig. 12 provides the ultrasonic pulse velocity (UPV) obtained for all the series with 28 days of curing. The control series had the greatest average velocity with a value of 4695 m/s, followed by the RCA-TC100 series with 4055 m/s and finally the RCA100 series with 3995 m/s. According to the Indian standard IS 13311–1 (IS 13311, 1992), the control series achieved an excellent quality for being over 4500 m/s, while the series with RCA for being over 3500 m/s were classified as good quality. It should also be noted that the pulse velocity was greater for the series with greater density due to the reduction in pores and empty spaces that make wave propagation difficult.

4.9. Thermogravimetric analysis (TGA)

Fig. 13 provides the derivative curves of the mass loss (DTG) during heating of the samples obtained from the thermogravimetric analysis (TGA) of all series after 28 days of curing. Due to the carbonation process used in this study, the peak of greatest importance occurs at 750 °C and corresponds to the dehydration of calcite in each sample (Castellote et al., 2009; Morandeau et al., 2014; Lu et al., 2019). As a result, the control series has a slight presence of this mineral, with a curve present

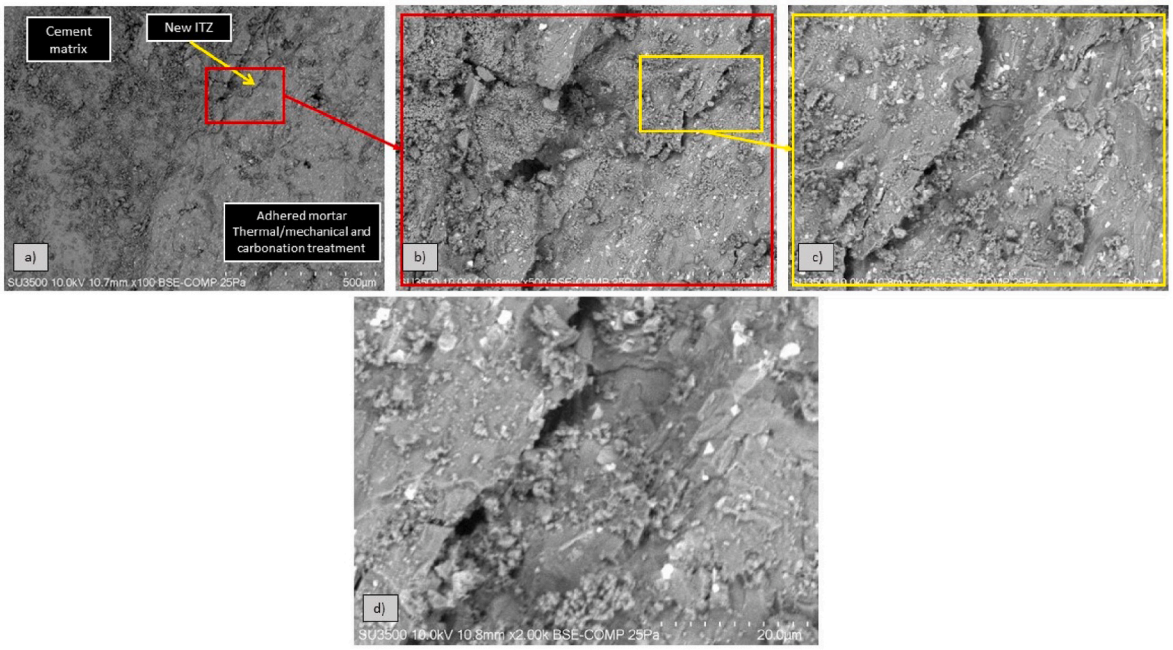

Fig. 8. SEM images of RCA-TC100 series.

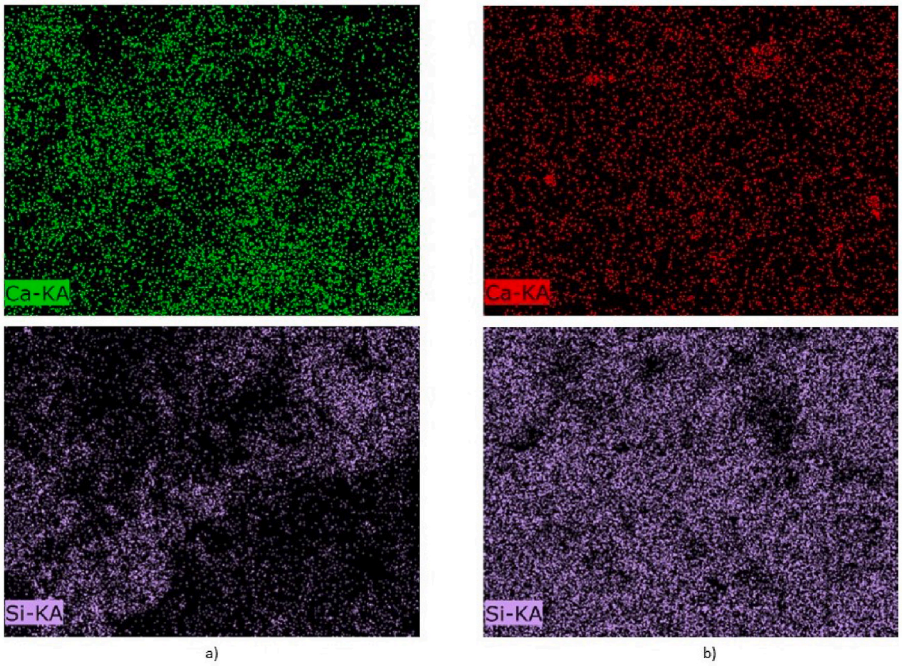

Fig. 9. MAPP of SEM images. (a) RCA100 series, and (b) RCA-TC100 series.

in a range of 645–735 °C, unlike the series with RCA that have more notable curves in the range of 715–770 °C. The control series has mass losses associated with calcite polymorphs (i.e., vaterite and aragonite) (Stepkowska et al., 2003), which may be due to the curing process of these samples, which could have led to a slight calcite precipitation after the 28 days of curing. On the other hand, and with mass losses of 2.18% and 2.12% for the RCA100 and RCA-TC100 series, respectively, this indicates the presence of calcite due to carbonation of the mineral produced for being in contact with the atmosphere in the case of RCA100 and in contact with the accelerated carbonation process for RCA-TC100. Although there is less presence of this mineral in the RCA-TC100 series, it must be remembered that the aggregates were subjected to a previous process (i.e., thermal and abrasion), which loosened the adhered mortar and dehydrated the compounds on their surface. Therefore, unlike the recycled aggregate, the carbon dioxide reacted with a smaller proportion of adhered mortar, and thus less portlandite.

This is related to what occurs at 460 °C, which is related to this mineral. Like the C–S–H, portlandite reacts with CO_2 to generate calcite (Castellote et al., 2009; Morandeau et al., 2014; Lu et al., 2019). This is why the C00 series presents a greater mass loss of this mineral than the other series. With respect to the series with incorporation of RCA from a

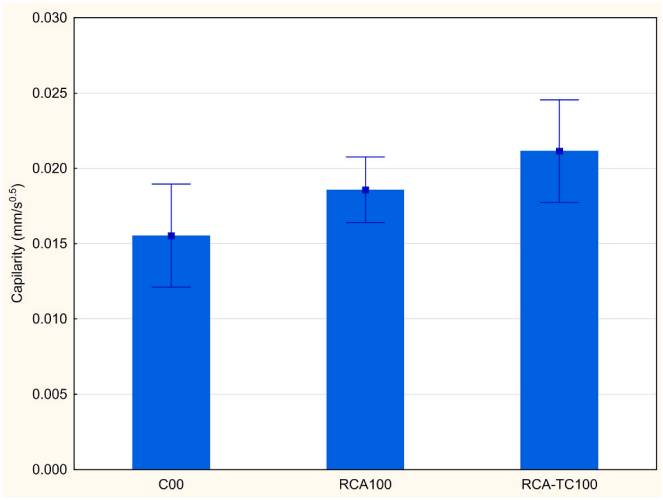

Fig. 10. Initial capillary absorption rate at 28 days.

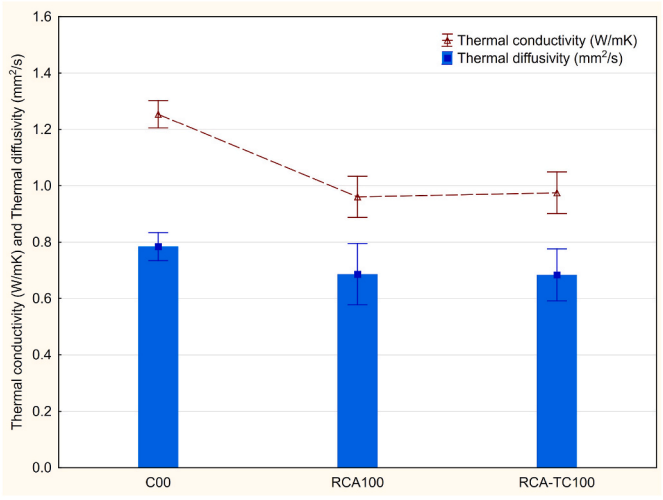

Fig. 11. Thermal conductivity and thermal diffusivity at 28 days.

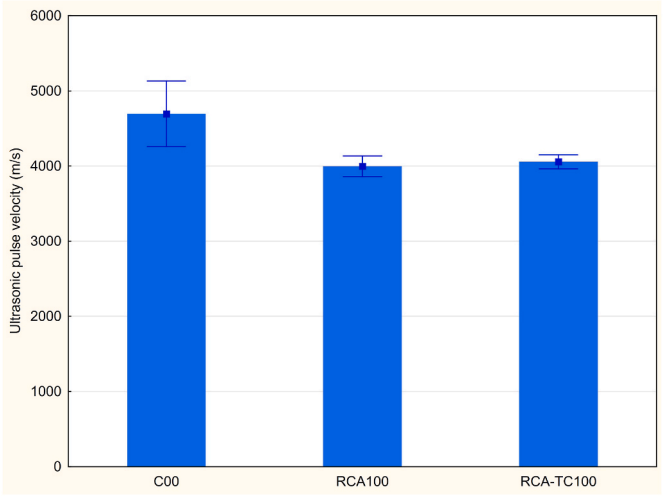

Fig. 12. Ultrasonic pulse velocity at 28 days.

concrete that was exposed to the environment in a landfill, the presence of portlandite in the RCA100 series is less, and in the same way for the RCA-TC100 series, where the aggregates were exhibited to carbon dioxide during the process.

The peak corresponding to the mass loss of hydrated components, linked to C–S–H, is found at 105 °C (Castellote et al., 2009). The C00 series had the greatest variation of C–S–H mass without carbonation, followed by the RCA100 series and then RCA-TC100. In addition, a slight peak present only for the series with treated RCA is observed, related to the phase change of the C–S–H due to accelerated carbonation, which thereby generates an amorphous and denser silica gel (Šavija and Luković, 2016). However, according to El-Hassan et al. (2013), mass loss in the amorphous or poorly crystallized range of the calcium carbonate appears between 550 °C and 720 °C. As previously indicated for the C00 series, the RCA100 series has more endothermic peaks than the RCA-TC series; therefore, the combination of improvement processes in the RCA-TC aggregate resulted in the precipitation of calcite with better crystallinity. Considering the absorption and porosity results, the improvement process resulted in a structure that, despite being equally porous, has a stronger matrix, thus explaining the best mechanical behavior despite both the absorption and porosity indicating minimal improvements.

4.10. XRD analysis

XRD analysis can be extracted from Fig. 14, which shows all the series studied at 28 days, where all the diffractograms present their highest peaks within the range of 2θ between 15° and 35°, but with some peaks appreciable up to 50°. In all the samples, there is evidence of quartz (Q), feldspar (F) and portlandite (P) in smaller amounts, components linked to the origin of the aggregates (Arivumangai et al., 2021) and to the hydration products of the cement used in the mixtures (Zhan et al., 2020; Šavija and Luković, 2016). In addition, the XRD diagrams indicate the existence of aragonite for the samples with natural carbonation as well as for accelerated carbonation. According to Morandeau et al. (2014), the formation of aragonite tends to be related to the presence of highly decalcified C–S–H, indicating elevated CO_2 concentrations.

In addition, there is a clear presence of calcite in the series with RCA, and which decreases for the control series. Similarly to the analyses performed by the TGA, the greatest calcite presence is confirmed in the RCA100 series rather than in the RCA-TC100 series. This phenomenon may be due to the elimination of adhered mortar resulting from the thermal/mechanical treatment, since the elimination of this material in turn causes the percentage of calcite to decrease due to the greater proportion of NA and smaller amount of previously naturally carbonated adhered mortar.

4.11. CO_2 uptake

Table 3 shows the results of the CO_2 uptake of concretes with the incorporation of recycled aggregates. Although the RCA-TC100 samples were treated with an accelerated carbonation process, the values associated with the decomposition of the calcite are less than 0.8% compared to the RCA100 sample. This may be because these aggregates were subjected to an abrasion process prior to the carbonation process, eliminating a large part of the adhered mortar capable of reacting with the CO_2. However, considering that the recycled aggregates from the RCA-TC100 sample contained less adhered mortar to react with the CO_2, its sequestration rate was very similar to normal recycled aggregates, thus indicating the penetration of the gas to the most internal surface of the aggregate.

On the other hand, as mentioned by Qin and Gao (2019), it is possible to differentiate two curves associated with the decomposition of the calcite, the former being poorly crystallized, and the latter having a better crystalline structure, with a more even molecular layout and a

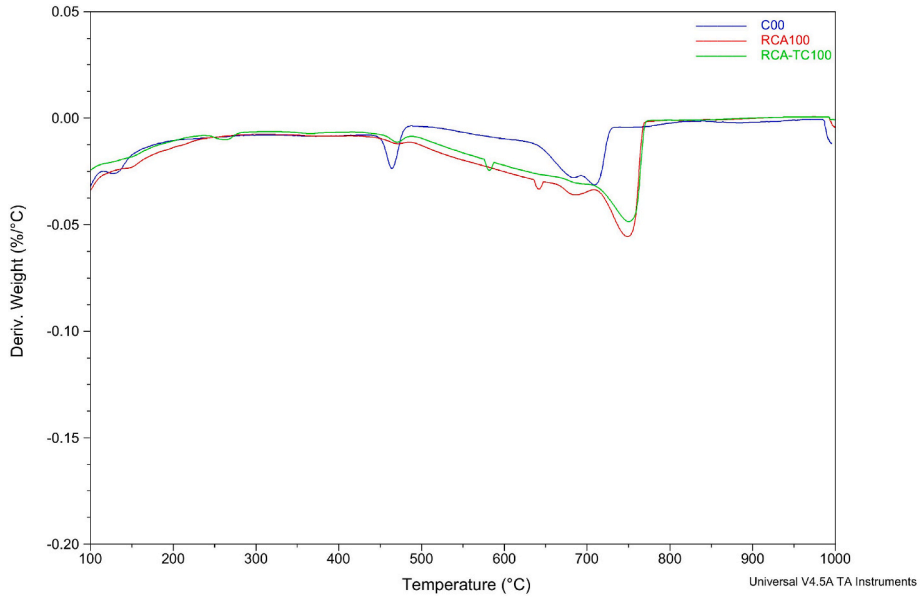

Fig. 13. DTG curve at 28 days.

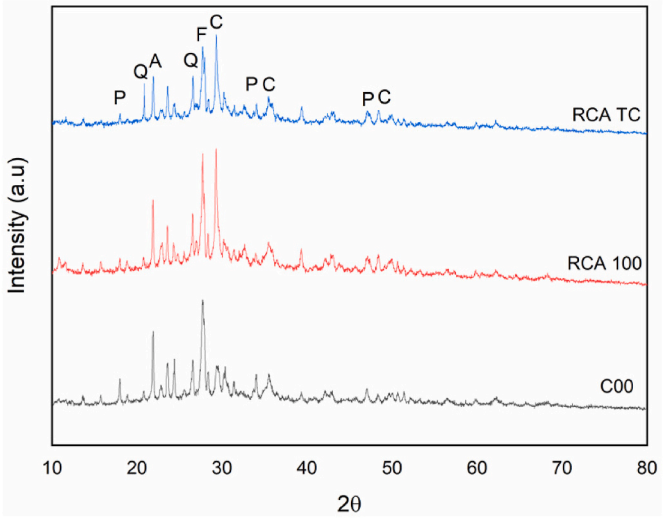

Fig. 14. X-ray diffraction at 28 days. A: aragonite, C: calcite, F: feldspar, P: portlandite, Q: quartz.

Table 3
CO_2 uptake of RCA concrete samples.

Sample	CO_2 (wt%)	$\Delta m_{540–720°C}$ (%)	$\Delta m_{720–950°C}$ (%)
RCA100	7.4	5.08	2.20
RCA-TC100	6.6	4.48	2.03

higher melting point (Shao et al., 2014; Tu et al., 2016). These decompositions occur in the range of 540–720 °C and 720–950 °C, respectively. In this sense, due to the exposure of the recycled aggregates to the atmosphere, the natural carbonation process resulted in obtaining calcite crystals of lower quality than those obtained in the aggregates subjected to the accelerated carbonation process, where there is a smaller percentage in the range of 540–720 °C.

Lastly, the combined treatment carried out could be a good option to maximize the use of recycled aggregates considering their nature, i.e. low-quality RCA partially carbonated under atmospheric exposure. However, initially the thermal treatment may be costly for large-scale applications, so it could be done by implementing new technologies or taking advantage of thermal processes from the manufacture of other products.

5. Conclusions

The main conclusions drawn from the results of the study of the total replacement of low-quality recycled aggregates partially carbonated due to weathering with thermal/mechanical treatment and accelerated carbonation in concretes have been summarized as follows.

- Both the CRA and the FRA had a positive result after the combined treatment, managing to increase the density by 2% and 3%, and to decrease the water absorption by 18% and 6% for the coarse and fine aggregate, respectively.
- The mechanical properties showed encouraging results, obtaining strengths at 28 days of the RAC close to the control series after the treatment, even with a considerably higher w/c ratio needed to maintain a flowable mix to meet the industry requirements, reaching 91% of the compressive strength and 96% of the flexural strength, indicating an improvement in the ITZ.
- The physical properties of the concrete had a negative impact when the NA was replaced by RCA, which can affect its durability. Even for a 100% replacement of coarse and fine aggregate, after the treatments used there was an improvement in the behavior of the RAC.
- The microstructural analysis using SEM and MAPP images reinforces the improvement obtained with the treatments used, showing a densification of the cement matrix with the aggregate thanks to the production of amorphous silica gel that filled the pores resulting from the carbonation of the C–S–H.
- The chemical results obtained from the DTG and XRD confirm what was observed in the physical tests and SEM images, and also confirmed the natural carbonation that the series with RCA possessed, showing greater calcite peaks.
- After accelerated carbonation, the calcite decomposition values were lower than for the untreated RCA, which could have occurred as a result of the thermal/mechanical process that removed a large part of the adhered mortar capable of reacting with the CO_2.
- The use of a single type of recycled aggregate presents limitations due to the variability in the properties of RCAs from different sources, which can affect the consistency of the results obtained;

therefore, the use of different aggregates should be considered in future studies to ensure representativeness.

CRediT authorship contribution statement

Bruno Wenzel: Conceptualization, Methodology, Writing – review & editing. **Viviana Letelier:** Conceptualization, Data curation, Funding acquisition, Investigation, Methodology, Supervision, Writing – review & editing. **Gonzalo Zambrano:** Data curation, Investigation, Writing – original draft. **Marión Bustamante:** Investigation, Methodology, Supervision. **José Marcos Ortega:** Conceptualization, Methodology.

Declaration of competing interest

The authors declare that they have no known competing financial interests or personal relationships that could have appeared to influence the work reported in this paper.

Data availability

Data will be made available on request.

Acknowledgement

This work was partially supported by Universidad de La Frontera (Chile) under Projects DI18-0023 and DI19-0019.

References

Al-Bayati, H.K.A., Das, P.K., Tighe, S.L., Baaj, H., 2016. Evaluation of various treatment methods for enhancing the physical and morphological properties of coarse recycled concrete aggregate. Construct. Build. Mater. 112, 284–298. https://doi.org/10.1016/j.conbuildmat.2016.02.176.

Alqarni, A.S., Abbas, H., Al-Shwikh, K.M., Al-Salloum, Y.A., 2021. Treatment of recycled concrete aggregate to enhance concrete performance. Construct. Build. Mater. 307, 124960 https://doi.org/10.1016/j.conbuildmat.2021.124960. URL: https://linkinghub.elsevier.com/retrieve/pii/S0950061821027100.

Arivumangai, A., Narayanan, R., Felixkala, T., 2021. Study on sulfate resistance behaviour of granite sand as fine aggregate in concrete through material testing and XRD analysis, 43, 1724–1729. https://doi.org/10.1016/j.matpr.2020.10.354. https://linkinghub.elsevier.com/retrieve/pii/S2214785320379748.

ASTM C127-15, 2015. Standard Test Method for Relative Density (Specific Gravity) and Absorption of Coarse Aggregate. ASTM International, West Conshohocken, PA.

ASTM C128-15, 2015. Standard Test Method for Relative Density (Specific Gravity), and Absorption of Fine Aggregate. ASTM International, West Conshohocken, PA.

ASTM C131/C131M-20, 2020. Standard Test Method for Resistance to Degradation of Small-Size Coarse Aggregate by Abrasion and Impact in the Los Angeles Machine. ASTM International, West Conshohocken, PA.

ASTM C1585-20, 2020. Standard Test Method for Measurement of Rate of Absorption of Water by Hydraulic Cement Concretes. ASTM International, West Conshohocken, PA.

ASTM C31/C31M-19, 2019. Standard Practice for Making and Curing Concrete Test Specimens in the Field. ASTM International, West Conshohocken, PA.

ASTM C39/C39M-21, 2021. Standard Test Method for Compressive Strength of Cylindrical Concrete Specimens. ASTM International, West Conshohocken, PA.

ASTM C469/C469M-14, 2014. Standard Test Method for Static Modulus of Elasticity and Poisson's Ratio Concrete in Compression. ASTM International, West Conshohocken, PA.

ASTM C494/C494M-19, 2019. Standard Specification for Chemical Admixtures for Concrete. ASTM International, West Conshohocken, PA.

ASTM C595/C595M-16, 2021. Standard Specification for Blended Hydraulic Cements. ASTM International, West Conshohocken, PA.

ASTM C597-16, 2016. Standard Test Method for Pulse Velocity through Concrete. ASTM International, West Conshohocken, PA.

ASTM C642-21, 2021. Standard Test Method for Density, Absorption, and Voids in Hardened Concrete. ASTM International, West Conshohocken, PA.

ASTM C78/C78M-18, 2018. Standard Test Method for Flexural Strength of Concrete (Using Simple Beam with Third-Point Loading). ASTM International, West Conshohocken, PA.

Biskri, Y., Achoura, D., Chelghoum, N., Mouret, M., 2017. Mechanical and durability characteristics of high performance concrete containing steel slag and crystalized slag as aggregates. Construct. Build. Mater. 150, 167–178. https://doi.org/10.1016/j.conbuildmat.2017.05.083.

Cao, Y., Wang, Y., Zhang, Z., Wang, H., 2022. Recycled sand from sandstone waste: a new source of high-quality fine aggregate. Resour. Conserv. Recycl. 179, 106116 https://doi.org/10.1016/j.resconrec.2021.106116. https://linkinghub.elsevier.com/retrieve/pii/S0921344921007242.

Carriço, A., Bogas, J.A., Guedes, M., 2020. Thermoactivated cementitious materials – a review. Construct. Build. Mater. 250, 118873 https://doi.org/10.1016/j.conbuildmat.2020.118873. URL: https://linkinghub.elsevier.com/retrieve/pii/S0950061820308783.

Castellote, M., Fernandez, L., Andrade, C., Alonso, C., 2009. Chemical changes and phase analysis of opc pastes carbonated at different co2 concentrations. Materials and Structures/Materiaux et Constructions 42, 515–525. https://doi.org/10.1617/s11527-008-9399-1.

David, T., Mike, van Acoleyen, Wouter, H., Tom, T., Carolien, van Brunschot, Brendan, E., Ben, K., 2018. SCALING the CIRCULAR BUILT ENVIRONMENT: Pathways for Bussiness Government.

El-Hassan, H., Shao, Y., Ghouleh, Z., 2013. Reaction products in carbonation-cured Lightweight concrete. J. Mater. Civ. Eng. 25, 799–809. URL: https://ascelibrary.org/doi/10.1061/%28ASCE%29MT.1943-5533.0000638.

Gholizadeh-Vayghan, A., Bellinkx, A., Snellings, R., Vandoren, B., Quaghebeur, M., 2020. The effects of carbonation conditions on the physical and microstructural properties of recycled concrete coarse aggregates. Construct. Build. Mater. 257, 119486 https://doi.org/10.1016/j.conbuildmat.2020.119486. https://linkinghub.elsevier.com/retrieve/pii/S0950061820314914.

Gonçalves, P., De Brito, J., 2010. Recycled aggregate concrete (RAC) - comparative analysis of existing specifications. Mag. Concr. Res. 62, 339–346. https://doi.org/10.1680/macr.2008.62.5.339.

Han, S.H., Jun, Y., Kim, J.H., 2023. The use of monoethanolamine CO2 solvent for the CO2 curing of cement-based materials. Sustainable Materials and Technologies 35, e00559. https://doi.org/10.1016/j.susmat.2022.e00559. https://linkinghub.elsevier.com/retrieve/pii/S2214993722001737.

Hyvert, N., Sellier, A., Duprat, F., Rougeau, P., Francisco, P., 2010. Dependency of c-s-h carbonation rate on co2 pressure to explain transition from accelerated tests to natural carbonation. Cement Concr. Res. 40, 1582–1589. https://doi.org/10.1016/j.cemconres.2010.06.010.

IS 13311-1, Method of Non-destructive Testing of Concrete, Part 1: Ultrasonic Pulse Velocity, 1992. Bureau of Indian Standards, Manak Bhawan, New Delhi.

Islam, R., Nazifa, T.H., Yuniarto, A., Uddin, A.S.S., Salmiati, S., Shahid, S., 2019. An empirical study of construction and demolition waste generation and implication of recycling. Waste Manag. 95, 10–21. https://doi.org/10.1016/j.wasman.2019.05.049.

ISO 22007-2:2008(E), 2008. Plastics - Determination of Thermal Conductivity and Thermal Diffusivity - Part 2: Transient Plane Heat Source (Hot Disc) Method. ISO, Geneva, CH.

Kaliyavaradhan, S.K., Ling, T.-C., Mo, K.H., 2020. CO2 sequestration of fresh concrete slurry waste: Optimization of CO2 uptake and feasible use as a potential cement binder. J. CO2 Util. 42, 101330 https://doi.org/10.1016/j.jcou.2020.101330. https://linkinghub.elsevier.com/retrieve/pii/S2212982020309604.

Kazmi, S.M.S., Munir, M.J., Wu, Y.-F., Patnaikuni, I., Zhou, Y., Xing, F., 2019. Influence of different treatment methods on the mechanical behavior of recycled aggregate concrete: a comparative study. Cement Concr. Compos. 104, 103398 https://doi.org/10.1016/j.cemconcomp.2019.103398. https://linkinghub.elsevier.com/retrieve/pii/S0958946519304226.

Kazmi, S.M.S., Munir, M.J., Wu, Y.-F., Patnaikuni, I., Zhou, Y., Xing, F., 2020. Effect of recycled aggregate treatment techniques on the durability of concrete: a comparative evaluation. Construct. Build. Mater. 264, 120284 https://doi.org/10.1016/j.conbuildmat.2020.120284. https://linkinghub.elsevier.com/retrieve/pii/S0950061820322893.

Kazmi, S.M.S., Munir, M.J., Wu, Y.-F., Lin, X., Ahmad, M.R., 2021. Investigation of thermal performance of concrete incorporating different types of recycled coarse aggregates. Construct. Build. Mater. 270, 121433 https://doi.org/10.1016/j.conbuildmat.2020.121433. https://linkinghub.elsevier.com/retrieve/pii/S0950061820334371.

Kou, S.-C., Zhan, B.-j., Poon, C.-S., 2014. Use of a CO2 curing step to improve the properties of concrete prepared with recycled aggregates. Cement Concr. Compos. 45, 22–28. https://doi.org/10.1016/j.cemconcomp.2013.09.008. https://linkinghub.elsevier.com/retrieve/pii/S0958946513001364.

Letelier, V., Bustamante, M., Muñoz, P., Rivas, S., Ortega, J.M., 2021. Evaluation of mortars with combined use of fine recycled aggregates and waste crumb rubber. J. Build. Eng. 43 https://doi.org/10.1016/j.jobe.2021.103226.

Liu, S., Shen, P., Xuan, D., Li, L., Sojobi, A., Zhan, B., Poon, C.S., 2021a. A comparison of liquid-solid and gas-solid accelerated carbonation for enhancement of recycled concrete aggregate. Cement Concr. Compos. 118 https://doi.org/10.1016/j.cemconcomp.2021.103988.

Liu, J., Fan, X., Liu, J., Jin, H., Zhu, J., Liu, W., 2021b. Investigation on mechanical and micro properties of concrete incorporating seawater and sea sand in carbonized environment. Construct. Build. Mater. 307, 124986 https://doi.org/10.1016/j.conbuildmat.2021.124986. https://linkinghub.elsevier.com/retrieve/pii/S0950061821027343.

Lu, B., Shi, C., Cao, Z., Guo, M., Zheng, J., 2019. Effect of carbonated coarse recycled concrete aggregate on the properties and microstructure of recycled concrete. J. Clean. Prod. 233, 421–428. https://doi.org/10.1016/j.jclepro.2019.05.350.

Makul, N., 2020. Modern sustainable cement and concrete composites: review of current status, challenges and guidelines. Sustainable Materials and Technologies 25, e00155. https://doi.org/10.1016/j.susmat.2020.e00155. https://linkinghub.elsevier.com/retrieve/pii/S2214993719303756.

Malešev, M., Radonjanin, V., Marinković, S., 2010. Recycled concrete as aggregate for structural concrete production. Sustainability 2, 1204–1225. https://doi.org/10.3390/su2051204.

Morandeau, A., Thiéry, M., Dangla, P., 2014. Investigation of the carbonation mechanism of ch and c-s-h in terms of kinetics, microstructure changes and moisture

properties. Cement Concr. Res. 56, 153–170. https://doi.org/10.1016/j.cemconres.2013.11.015.
Munir, M.J., Kazmi, S.M.S., Wu, Y.-F., Lin, X., 2021. Axial stress-strain performance of steel spiral confined acetic acid immersed and mechanically rubbed recycled aggregate concrete. J. Build. Eng. 34, 101891 https://doi.org/10.1016/j.jobe.2020.101891. https://linkinghub.elsevier.com/retrieve/pii/S2352710220335245.
Neville, A.M., 1995. In: Properties of Concrete, vol. 4. Longman London.
OECD, European Commission, 2020. Cities in the world: a new Perspective on Urbanisation. URL: https://www.oecd-ilibrary.org/content/publication/d0efcbda-en. https://doi.org/10.1787/d0efcbda-en.
Pandurangan, K., Dayanithy, A., Prakash, S.O., 2016. Influence of treatment methods on the bond strength of recycled aggregate concrete. Construct. Build. Mater. 120, 212–221. https://doi.org/10.1016/j.conbuildmat.2016.05.093.
Pepe, M., Toledo Filho, R.D., Koenders, E.A., Martinelli, E., 2014. Alternative processing procedures for recycled aggregates in structural concrete. Construct. Build. Mater. 69, 124–132. https://doi.org/10.1016/j.conbuildmat.2014.06.084. https://linkinghub.elsevier.com/retrieve/pii/S095006181400703X.
Prajapati, R., Gettu, R., Singh, S., 2021. Thermomechanical beneficiation of recycled concrete aggregates (RCA). Construct. Build. Mater. 310, 125200 https://doi.org/10.1016/j.conbuildmat.2021.125200. https://linkinghub.elsevier.com/retrieve/pii/S0950061821029445.
Qin, L., Gao, X., 2019. Recycling of waste autoclaved aerated concrete powder in Portland cement by accelerated carbonation. Waste Manag. 89, 254–264. https://doi.org/10.1016/j.wasman.2019.04.018. https://linkinghub.elsevier.com/retrieve/pii/S0956053X19302314.
Robalo, K., Costa, H., do Carmo, R., Júlio, E., 2021. Experimental development of low cement content and recycled construction and demolition waste aggregates concrete. Construct. Build. Mater. 273, 121680 https://doi.org/10.1016/j.conbuildmat.2020.121680. URL: https://linkinghub.elsevier.com/retrieve/pii/S0950061820336849.
Rostami, J., Khandel, O., Sedighardekani, R., Sahneh, A.R., Ghahari, S.A., 2021. Enhanced workability, durability, and thermal properties of cement-based composites with aerogel and paraffin coated recycled aggregates. J. Clean. Prod. 297, 126518 https://doi.org/10.1016/j.jclepro.2021.126518. URL: https://linkinghub.elsevier.com/retrieve/pii/S0959652621007381.
Šavija, B., Luković, M., 2016. Carbonation of cement paste: Understanding, challenges, and opportunities. Construct. Build. Mater. 117, 285–301. https://doi.org/10.1016/j.conbuildmat.2016.04.138.
Shao, Y., Rostami, V., He, Z., Boyd, A.J., 2014. Accelerated carbonation of Portland limestone cement. J. Mater. Civ. Eng. 26, 117–124. URL: https://ascelibrary.org/doi/10.1061/%28ASCE%29MT.1943-5533.0000773.
Shi, C., Wu, Z., Cao, Z., Ling, T.C., Zheng, J., 2018. Performance of mortar prepared with recycled concrete aggregate enhanced by co2 and pozzolan slurry. Cement Concr. Compos. 86, 130–138. https://doi.org/10.1016/j.cemconcomp.2017.10.013.
Shui, Z., Xuan, D., Chen, W., Yu, R., Zhang, R., 2009. Cementitious characteristics of hydrated cement paste subjected to various dehydration temperatures. Construct. Build. Mater. 23, 531–537. https://doi.org/10.1016/j.conbuildmat.2007.10.016.
Stepkowska, E.T., Pérez-Rodríguez, J.L., Sayagués, M.J., Martínez-Blanes, J.M., 2003. Calcite, vaterite and aragonite forming on cement hydration from liquid and gaseous phase. J. Therm. Anal. Calorim. 73, 247–269. https://doi.org/10.1023/A:1025158213560.
Sui, Y., Mueller, A., 2012. Development of thermo-mechanical treatment for recycling of used concrete. Mater. Struct. 45, 1487–1495. URL: http://link.springer.com/10.1617/s11527-012-9852-z.
Tam, V.W., Soomro, M., Evangelista, A.C.J., 2021. Quality improvement of recycled concrete aggregate by removal of residual mortar: a comprehensive review of approaches adopted. Construct. Build. Mater. 288 https://doi.org/10.1016/j.conbuildmat.2021.123066.
Tanta, A., Kanoungo, A., Singh, S., Kanoungo, S., 2022. The effects of surface treatment methods on properties of recycled concrete aggregates. Mater. Today: Proc. 50, 1848–1852. https://doi.org/10.1016/j.matpr.2021.09.223. URL: https://linkinghub.elsevier.com/retrieve/pii/S221478532106065X.
Thomas, J., Thaickavil, N.N., Wilson, P.M., 2018. Strength and durability of concrete containing recycled concrete aggregates. J. Build. Eng. 19, 349–365. https://doi.org/10.1016/j.jobe.2018.05.007.
Tu, Z., Guo, M.Z., Poon, C.S., Shi, C., 2016. Effects of limestone powder on CaCO3 precipitation in CO2 cured cement pastes. Cement Concr. Compos. 72, 9–16. https://doi.org/10.1016/j.cemconcomp.2016.05.019.
Wang, C., Xiao, J., Zhang, G., Li, L., 2016. Interfacial properties of modeled recycled aggregate concrete modified by carbonation. Construct. Build. Mater. 105, 307–320. https://doi.org/10.1016/j.conbuildmat.2015.12.077.
Wang, W., Xiao, J., Xu, S., Wang, C., 2017. Experimental study on behavior of mortar-aggregate interface after elevated temperatures. Front. Struct. Civ. Eng. 11, 158–168. URL: http://link.springer.com/10.1007/s11709-016-0374-6.
Wang, D., Xiao, J., Duan, Z., 2022. Strategies to accelerate co2 sequestration of cement-based materials and their application prospects. Construct. Build. Mater. 314 https://doi.org/10.1016/j.conbuildmat.2021.125646.
Xuan, D., Zhan, B., Poon, C.S., 2016. Assessment of mechanical properties of concrete incorporating carbonated recycled concrete aggregates. Cement Concr. Compos. 65, 67–74. https://doi.org/10.1016/j.cemconcomp.2015.10.018.
Xuan, D., Zhan, B., Poon, C.S., 2017. Durability of recycled aggregate concrete prepared with carbonated recycled concrete aggregates. Cement Concr. Compos. 84, 214–221. https://doi.org/10.1016/j.cemconcomp.2017.09.015.
Zadeh, A.H., Mamirov, M., Kim, S., Hu, J., 2021. Co2-treatment of recycled concrete aggregates to improve mechanical and environmental properties for unbound applications. Construct. Build. Mater. 275 https://doi.org/10.1016/j.conbuildmat.2020.122180.
Zega, C.J., Maio, A.A.D., 2009. Recycled concrete made with different natural coarse aggregates exposed to high temperature. Construct. Build. Mater. 23, 2047–2052. https://doi.org/10.1016/j.conbuildmat.2008.08.017.
Zhan, B., Poon, C.S., Liu, Q., Kou, S., Shi, C., 2014. Experimental study on co2 curing for enhancement of recycled aggregate properties. Construct. Build. Mater. 67, 3–7. https://doi.org/10.1016/j.conbuildmat.2013.09.008.
Zhan, B.J., Xuan, D.X., Poon, C.S., Scrivener, K.L., 2020. Characterization of interfacial transition zone in concrete prepared with carbonated modeled recycled concrete aggregates. Cement Concr. Res. 136 https://doi.org/10.1016/j.cemconres.2020.106175.
Zhang, D., Ghouleh, Z., Shao, Y., 2017. Review on carbonation curing of cement-based materials. J. CO2 Util. 21, 119–131. https://doi.org/10.1016/j.jcou.2017.07.003. https://linkinghub.elsevier.com/retrieve/pii/S2212982017302524.
Zhang, H., Wei, W., Shao, Z., Qiao, R., 2022. The investigation of concrete damage and recycled aggregate properties under microwave and conventional heating. Construct. Build. Mater. 341, 127859 https://doi.org/10.1016/j.conbuildmat.2022.127859. https://linkinghub.elsevier.com/retrieve/pii/S095006182201532X.